Cascaded nonlinearity and two-color solitons in photonic band-gap fibres filled with a Raman active gas

F. Biancalana, D.V. Skryabin, D.M. Bird and F. Benabid
Department of Physics, University of Bath, Bath BA2 7AY, UK
(June 1, 2004)

We report the existence of two-color, temporal bright-bright and dark-bright solitons supported by effective Kerr nonlinearity in hollow-core photonic crystal fibres filled with a Raman active gas and demonstrate the feasibility of their experimental observation.

Control of light using photonic crystals is becoming increasingly important in science and technology. In particular, applications of photonic crystal fibres (PCFs) [1] in nonlinear optics have attracted significant recent attention, see, e.g., [2–4]. Hollow-core band-gap guiding PCFs [1,4,9] filled with gases offer various opportunities for investigation of nonlinear effects in gases in conditions where undesirable diffraction is cancelled, losses are small and the useful interaction length is greatly increased compared to the more conventional use of capillaries and gas cells. Recent observations of the low-threshold generation of Raman side-bands in hydrogen-filled PCF [3] and of Kerr solitons in fibres with air and xenon [4] have been the first results in this promising area of research.

Designing methods of controlling nonlinearities is one of the long standing challenges in optics. A well known example of an artificial nonlinearity is the effective or cascaded Kerr nonlinearity induced by the second harmonic in materials with quadratic nonlinearity [5]. Another example of a similar nonlinearity occurs in Raman active materials which are driven by two fields with the frequency difference detuned from the frequency of the Raman transition [6,7]. The strength of the effective nonlinearities can be orders of magnitude larger than of the intrinsic Kerr nonlinearity. Here we suggest the use of a hollow-core PCF filled with a Raman active gas pumped by two-color pulses for creating an effective nonlinearity which exceeds the intrinsic Kerr nonlinearity of such fibres by two orders of magnitude. We propose to use this system for the observation of various two-color temporal solitons at peak powers of order 10kW, which is well below the megawatt peak powers needed to observe solitons due to intrinsic nonlinearities [4].

The use of short pulses for inducing effective nonlinearity is preferred over the use of a continuous wave [7], due to the power limitations of the latter. The danger here, however, is that pulses propagating at different group velocities will simply walk through one another, quickly destroying the induced nonlinearity. However, as we show below, photonic band-gap fibres offer unique opportunities to match the group velocities of the fundamental fibre modes and even adjust the fibre dispersion to achieve the matching for the required frequencies. It is also important that the group velocity matching in these fibres can take place when the group velocity dispersions (GVDs) of the interacting fields have the same sign. This creates an ideal environment for the observation of temporal bright-bright solitons [8].

We consider the PCF shown in Figs. 1b and 1c with the pitch between the air holes equal to Λ and the strut thickness 0.03Λ. This structure is very similar to the PCFs used in experiments [4,9]. Dispersion of the PCF modes can be characterized by the dependence of $\beta\Lambda$ on $\nu = k\Lambda$, where $\beta(\omega)$ is the propagation constant, k is vacuum wavenumber, $\omega = c\nu/\Lambda$ is the angular frequency, and $c = 3\times10^8$ m/s. The group velocity is given by $1/\beta_1$, see Fig. 1(a), where $\beta_1 = \partial_\omega\beta = c^{-1}d(\beta\Lambda)/d\nu$. An important feature of the PCF under consideration and of the ones used in [4,9] is the presence of one or more high loss spectral windows where the dynamics is dominated by the surface modes localized around the walls of the fibre core, see [9] and Fig. 1(a). As a result of this the photonic band gap has several branches of the fundamental modes and each branch has a point where the GVD, $\beta_2 = \partial_\omega\beta_1$, is zero. Clearly, the dispersion characteristic in Fig. 1(a) offers several opportunities to match the group velocities of the two pulses. Moreover, if the group velocities at ν_1 and ν_2 are matched then the corresponding frequency difference is given by $\Delta = c(\nu_1 - \nu_2)/\Lambda$ and a fibre with the pitch required to achieve the group velocity matching for a given Δ can be fabricated.

We consider the above PCF filled with a Raman active gas and pumped by two pulses with a frequency difference $\Delta = (\omega_1 - \omega_2) > 0$ detuned from the frequency ω_r of the Raman resonance, i.e. $\omega_r - \Delta \neq 0$. Dimensionless equations describing this process are

$$i\partial_z E_1 = iv\partial_t E_1 - d_1\partial_t^2 E_1 - \kappa E_2 Q, \tag{1}$$
$$i\partial_z E_2 = -iv\partial_t E_2 - d_2\partial_t^2 E_2 - \kappa E_1 Q^*, \tag{2}$$
$$0 = i\partial_t Q + (\delta + i\epsilon)Q + \kappa E_1 E_2^*. \tag{3}$$

Eqs. (1-3) describe the simplest situation, when the Raman transition is not saturated and energy transfer to the higher-order Stokes and anti-Stokes components either does not happen or can be disregarded [7,10]. Q is the Raman coherence and κ is the dimensionless coupling constant, the choice of which is determined by the choice of the normalization of the slowly varying amplitudes $E_{1,2}$ and Q. Dimensionless delay t is measured in the units of the characteristic pulse duration τ, and the propagation distance z is in the units of the GVD length $l_{gvd} = \tau^2/|\beta^{(2)}(\omega_2)|$. Then $d_2 = sgn(\beta^{(2)}(\omega_2))$ and $d_1 = \beta^{(2)}(\omega_1)/|\beta^{(2)}(\omega_2)|$ is the ratio of the GVDs of the fields. δ is the normalized detuning of the frequency difference of the driving fields from the Raman resonance frequency ω_r, i.e. $\delta = \tau(\omega_r - \Delta)$. $\epsilon = \tau/T_2$, where $1/T_2$ is the width of the Raman resonance. The parameter v characterizes the difference of the group velocities of the driving fields and it is expressed as half of the ratio of the GVD length and of the walk-off length $l_{gvm} = \tau/[\beta^{(1)}(\omega_2) - \beta^{(1)}(\omega_1)]$: $v = l_{gvd}/(2l_{gvm})$.

Throughout this work we consider the situation of a large Raman detuning: $|\delta| \gg 1$ and $|\delta| \gg \epsilon$. Then by neglecting ϵ we derive an approximate solution for the coherence

$$Q = -\frac{\kappa}{\delta}\left[1 - \frac{i}{\delta}\partial_t + O(|\delta|^{-2})\right] E_1 E_2^*. \quad (4)$$

By substituting (4) into Eqs. (1),(2) one can derive nonlinearly coupled Schrödinger equations. An important property of these equations is that they do not have nonlinear self-phase modulation terms [11]. For $\delta > 0$ the effective nonlinearity is focusing and for $\delta < 0$ it is defocusing. If one compares Eqs. (1-3) with the system used to study temporal Raman solitons in gas cells [10], then the difference is that $v = d_{1,2} = \delta = 0$ in the latter, which makes the physical origin and properties of the solitons described in [10] completely different from our case.

It is convenient here to adopt the standard normalization used in the fibre optics, when physical fields are normalized to the square root of the so-called nonlinear fibre parameter γ [11]. This is achieved by choosing $\kappa = |\delta|^{1/2}$. Let us now derive an expression for γ_{eff}, which is the nonlinear parameter due to the effective Kerr nonlinearity. One can verify that $|\delta|/(\delta^2 + \epsilon^2) = C\gamma_{eff}$, where C is some proportionality coefficient. Using the definition of the steady-state Raman gain at the line centre, g_{ss}, see [10], one can verify that $\epsilon/(\delta^2 + \epsilon^2) = Cg_{ss}/A/(1 + T_2^2|\omega_r - \Delta|^2)$, where A is the area of the fiber mode. In the limit of a large detuning from the Raman resonance the last two expressions give:

$$\gamma_{eff} \simeq \frac{g_{ss}}{A} \times \frac{1}{T_2|\omega_r - \Delta|}. \quad (5)$$

We now turn our attention to the soliton solutions of Eqs. (1), (2) and (4). By analogy with other two component systems [11,12] we expect that these solitons can be parameterized by three independent parameters associated with invariances with respect to the two phase rotations, $E_{1,2} \to E_{1,2}e^{i\psi_{1,2}}$ and translations of t. We neglect terms of $O(|\delta|^{-2})$ in Eq. (4) and seek solitons of the form $E_{1,2} = f_{1,2}(\xi)e^{-iq_{1,2}z}$, where $\xi = \tau - Vz$ and V is a parameter [12]. We have solved the system of ordinary differential equations for the functions $f_{1,2}$ numerically and have identified the existence of three distinct soliton families: bright-bright, bright-dark and dark-dark soliton pairs. Below we analyse only the bright-bright and bright-dark solitons.

Bright-bright solitons are likely to be the easiest to excite and observe in future experiments. They can exist either when the GVDs at both frequencies are anomalous ($d_{1,2} < 0$) and the effective nonlinearity is focusing ($\delta > 0$) or when the GVDs are normal ($d_{1,2} > 0$) and the nonlinearity is defocusing ($\delta < 0$). The decay rates of the tails of the bright-bright solitons are given by $\lambda_{1,2} = \sqrt{4q_{1,2}|d_{1,2}| - (v \pm V)^2}/|2d_{1,2}|$ and the solitons exist providing $Im\lambda_{1,2} = 0$. Linking parameters $q_{1,2}$ and V by the condition that the tails of both components decay with the same rate i.e. $\lambda_1 = \lambda_2$ and taking $Q = -sE_1E_2^*/\kappa$, where $s = sgn(\delta)$, we have found the explicit form of the bright-bright solitons:

$$E_{1,2} = a_{1,2}\exp\left\{i\xi\frac{V \pm v}{2d_{1,2}} - iq_{1,2}z\right\} sech\frac{\xi}{w}. \quad (6)$$

Here $w = \sqrt{-2sd_2}/a_1$, $a_2 = a_1\sqrt{d_1/d_2}$ and

$$a_1^2 = \frac{2|d_2|}{|d_1|}\left\{sq_1 - \frac{(V+v)^2}{4|d_1|}\right\}. \quad (7)$$

For (6) to be a good approximate solution to the exact system (1-3) we require that $|\partial_t E_1^* E_2| \ll |\delta|$. This condition ensures that the second term in the expansion (4) is much less than the first and it is satisfied for the soliton (6) if

$$|d_2(V + v) - d_1(V - v)| \ll 2|\delta d_1 d_2|. \quad (8)$$

Also it is clear at the intuitive level that if the walk-off length l_{gvm} becomes equal to or smaller than l_{gvd}, then it can greatly complicate the practical observation of the two-color solitons, because the two pulses will tend to separate spatially quicker than GVD can be compensated by nonlinearity. As is clear from Fig. 1(a), the matching of group velocities for two fields having GVDs of the same sign is possible only between the two branches of the fundamental mode.

From the Raman active gases we have chosen SF_6 as our working example. SF_6 has $\omega_r \simeq 2\pi \times 23$THz, which easily fits into the photonic band gap for typical values of Λ. The gain coefficient for SF_6 is $g_{ss} \simeq 14 \times 10^{-14}$m/W. Recent experiments with SF_6, where the symmetric vibrational Raman mode has been excited in hollow waveguides [14], have shown values of T_2 of order several ps's. Choosing $\tau = 1$ps, $T_2 = 1$ps, and detuning from the resonance $\omega_r - \Delta \equiv \alpha/T_2$, where α is a number, we find that $\delta = \alpha$ and $\epsilon = 1$. For example, taking $\Delta = 2\pi \times 24.6$THz gives $\alpha \simeq -10$ and we have $|\delta| \gg 1$, $|\delta| \gg \epsilon$. Negative values of δ imply defocusing nonlinearity and require normal GVDs for the bright solitons to exist. Choosing, for example, $\lambda_1 = 1.2712\mu m$ we achieve group velocity matching with the second pulse at $\lambda_2 = 1.1538\mu m$ for $\Lambda = 3\mu m$. These $\Lambda/\lambda_{1,2}$ values correspond to the modes shown in Figs. 1(b,c). Corresponding values of β_2 are $1.2\mathrm{ps}^2/\mathrm{m}$ for λ_1 and $0.4\mathrm{ps}^2/\mathrm{m}$ for λ_2. Despite the fact that we are detuned by 10 line-widths from the resonance, we have $\gamma_{eff} \simeq 10^{-4}\mathrm{W}^{-1}\mathrm{m}^{-1}$, which is two orders of magnitude larger than the value of γ due to intrinsic Kerr nonlinearities: $\gamma_{intr} \simeq 10^{-6}\mathrm{W}^{-1}\mathrm{m}^{-1}$ [4]. Thus our neglecting the intrinsic Kerr nonlinearity, which otherwise would give self-phase modulation terms in Eqs. (1) and (2), is well justified for the conditions discussed in this work. Also it follows that the observation of solitons due to effective nonlinearity requires peak powers of order 10kW only, and not of order 1MW as in [4].

One of the prime conditions for observation of solitons is their robustness against the growth of small perturbations. We have studied the stability of bright-bright solitons using the linearization of Eqs. (1,2,4) and their direct numerical simulation and have not found any instabilities, though the range of parameters is too wide to completely eliminate their existence. The existence and stability of these solitons within the full model (1-3) is a more delicate problem, though. Considering Eq. (3), one can easily observe that, in the linear approximation and for $\epsilon = 0$, Q does not decay to zero for $t \to \pm\infty$. Nevertheless solving Eqs. (1-3) numerically with the initial conditions (6) we have found that if the group velocities are exactly matched, then these approximate solitons quickly adjust to the full model and propagate without disturbance for many l_{gvd}, see Figs. 2(a-c). This suggests that nonlinear terms contribute strongly to the localization of Q. Small values of the parameter v, ensuring that the condition (8) is well satisfied, also do not alter the stability of the solitons. However, introducing a moderate mismatch of the group velocities, which starts to endanger condition (8), leads to a strong outburst of material excitation and destruction of the soliton, see Figs. 2(d-f). Dynamics of dark-bright solitons also will be reported, see Figs. 2(g-i).

[1] P.St.J. Russell, Science **299**, 358 (2003).

[2] J.K. Ranka, R.S. Windeler, and A.J. Stentz, Opt.Lett. **25**, 25 (2000); J. Herrmann *et al.*, Phys. Rev. Lett. **88**, 173901 (2002); W.H. Reeves *et al.*, Nature **424**, 511 (2003); D.V. Skryabin *et al.*, Science **301**, 1705 (2003).

[3] F. Benabid *et al.*, Science **298**, 399 (2002).

[4] D.G. Ouzounov *et al.*, Science **301**, 1702 (2003); F. Luan *et al.*, Opt. Exp. **12**, 835 (2004).

[5] For a review see G.I. Stegeman, Quantum and Semiclassical Opt. **9**, 139 (1997).

[6] A.V. Sokolov and S.E. Harris, J. Opt. B **5**, 1 (2003).

[7] D.D. Yavuz, D.R. Walker, and M.Y. Shverdin, Phys. Rev. A **67**, 041803 (2003); M.Y. Shverdin, D.D. Yavuz, and D.R. Walker, Phys. Rev. A **69**, 031801 (2004).

[8] A complicated experimental technique of dispersion manipulation, leading to the formation of temporal two frequency solitons in bulk quadratically nonlinear crystals, is described in P. Di Trapani *et al.*, Phys. Rev. Lett. **81**, 570 (1998).

[9] C.M. Smith *et al.*, Nature **424**, 657 (2003).

[10] K.J. Druhl, R.G. Wenzel, and J.L. Carlsten, Phys. Rev. Lett. **51**, 1171 (1983); J. Reintjes and M. Bashkansky, *in Handbook of Optics, vol. IV* ed. M. Bass (McGraw-Hill, NY, 2001), Chap. 18.

[11] Y.S. Kivshar and G.P. Agrawal, *Optical Solitons* (Academic Press, San Diego, 2003).

[12] Y.S. Kivshar and B. Luther-Davies, Phys. Rep. **298**, 81 (1998); A.V. Buryak, P. Di Trapani, D.V. Skryabin, and S. Trillo, Phys. Rep. **370**, 63 (2002).

[13] S. Trillo, S. Wabnitz, E.M. Wright, and G.I. Stegeman, Opt. Lett. **13**, 871 (1988).

[14] M. Wittman, A. Nazarkin, and G. Korn, Phys. Rev. Lett. **84**, 5508 (2000).

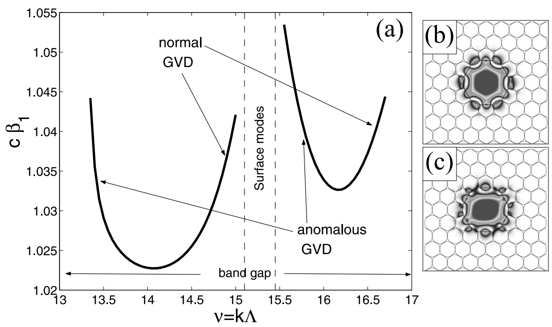

FIG. 1. (a) Ratio of the speed of light in vacuum to the group velocity of the fundamental PCF mode vs $k\Lambda$. Fundamental mode of the PCF for (b) $k\Lambda = 14.828$ and (c) $k\Lambda = 16.337$.

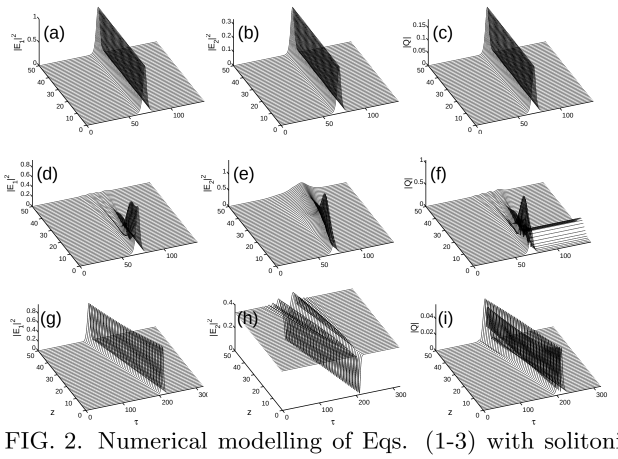

FIG. 2. Numerical modelling of Eqs. (1-3) with solitonic initial conditions (6) and (**??**-**??**). (a-c) Bright-bright soliton $d_1 = 1$, $d_2 = 3$, $s = -1$, $q_1 = 10$, $v = V = 0$. (d-f) The same as (a-c) but for $v = 3$. (g-i) Inverted dark-bright soliton. $d_1 = 1$, $d_2 = -3$, $s = 1$, $v = 3$, $q_1 = 10$, $\phi = V = 0$.